Electrochemistry
The Electrochemical Society of Japan
Received: November 15, 2021
Accepted: December 7, 2021
Published online: December 10, 2021
Issued: January 15, 2022
https://doi.org/10.5796/electrochemistry.21-00118
https://doi.org/10.50892/data.electrochemistry.17149778
Article
Electrochemistry, **90(1)**, 017011 (2022)

Impact of Hydrogen Peroxide on Carbon Corrosion in Aqueous KOH Solution

Atsunori IKEZAWA,[a,b,*,§] Kohei MIYAZAKI,[a,c,§] Tomokazu FUKUTSUKA,[a,c,§] and Takeshi ABE[a,c,§]

[a] *Graduate School of Engineering, Kyoto University, Nishikyo-ku, Kyoto 615-8510, Japan*
[b] *School of Materials and Chemical Technology, Tokyo Institute of Technology, Midori-ku, Yokohama 226-8502, Japan*
[c] *Hall of Global Environmental Research, Kyoto University, Nishikyo-ku, Kyoto 615-8510, Japan*

* *Corresponding author: ikezawa.a.aa@m.titech.ac.jp*

ABSTRACT

Impact of hydrogen peroxide on carbon corrosion is investigated by immersion tests of catalyst-deposited highly oriented pyrolytic graphite (HOPG) samples to an aqueous solution of 1.0 mol dm^{-3} KOH + 5 mmol dm^{-3} H_2O_2. The surfaces of the HOPG samples are observed with field-emission scanning electron microscopy and X-ray photoelectron spectroscopy. HOPG without catalyst shows almost no morphological change while the distribution of C-O and C=O functional groups increases. In contrast, Pt-loaded HOPG exhibits the formation of scars and COO functional groups, which shows a relatively severe carbon corrosion reaction resulting in CO_3^{2-} formation. Since the Pt-loaded HOPG after the immersion test to 0.5 mol dm^{-3} H_2SO_4 + 5 mmol dm^{-3} H_2O_2 shows much smaller scars, it can be concluded that hydrogen peroxide corrodes Pt-loaded carbon more severely in the alkaline electrolyte solution than the acid electrolyte solution. Ag-loaded HOPG also shows the scars, while the sizes of scars are much smaller than those on the Pt-loaded HOPG. In contrast, MnO_x and CoO_x-loaded HOPGs exhibit no scar and minor oxygen-containing functional groups than the HOPG without catalyst, whereas MnO_x and CoO_x-loaded HOPGs shows larger scars than Pt and Ag-loaded HOPGs after electrochemical carbon corrosion test.

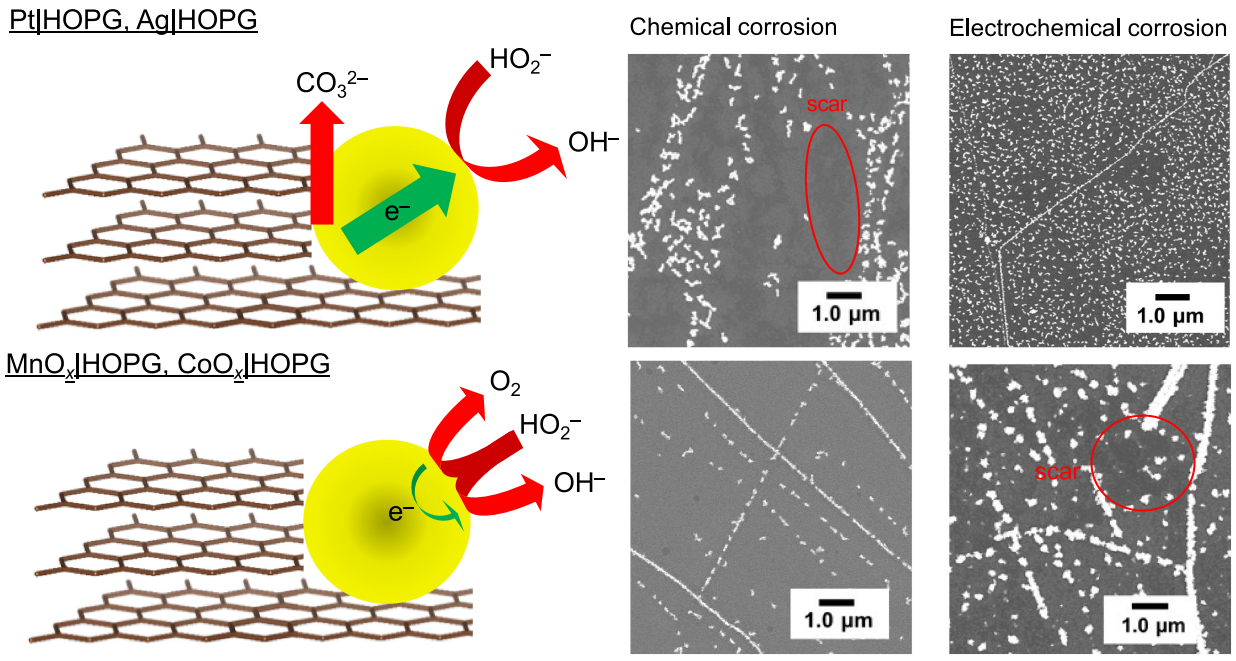

Keywords : Carbon Corrosion, Hydrogen Peroxide, Air Electrode, Metal-air Battery

1. Introduction

Alkaline air electrodes have attracted increasing attention as cathodes for alkaline fuel cells, chlor-alkali processes, and metal-air batteries.[1–3] These electrode systems potentially have lower costs than acid systems owing to the broader choices of catalysts, including low-cost nonprecious metal oxide catalysts. Toward their wider use, an improvement in durability is a crucial problem. One of the factors that limit the durability of the alkaline air electrode is carbon corrosion. High surface area carbons, such as carbon black, are usually used as catalyst support materials for air electrodes to provide adequate reaction sites and electronic conductivity. It is known that their surfaces are filled with oxygen-containing functional groups and etched to form CO_3^{2-} during the operations,

§ECSJ Active Member
A. Ikezawa orcid.org/0000-0002-8857-7159
K. Miyazaki orcid.org/0000-0001-5177-3570
T. Fukutsuka orcid.org/0000-0002-8731-9078
T. Abe orcid.org/0000-0002-1515-8340

which leads to the flooding and the loss of the active sites in air electrodes.[4–7]

There are two types of carbon corrosion reactions in alkaline air electrodes. The first one is an electrochemical carbon corrosion reaction, which comes from the much higher potential of the air electrode reaction (Eq. 1) than that of the carbon corrosion reaction (Eq. 2).[8]

$$O_2 + 2H_2O + 4e^- = 4OH^- \quad E^0 = 0.401\,\text{V vs. SHE} \quad (1)$$

$$CO_3^{2-} + 3H_2O + 4e^- = C + 6OH^-$$
$$E^0 = -0.584\,\text{V vs. SHE} \quad (2)$$

The second one is a chemical reaction induced by the strong oxidizability of hydrogen peroxide (HO_2^-): a stable intermediate product of oxygen reduction reaction (ORR) (Eq. 3).[9,10]

$$O_2 + H_2O + 2e^- = OH^- + HO_2^-$$
$$E^0 = -0.056\,\text{V vs. SHE} \quad (3)$$

In the acid electrolyte solution, Kinumoto et al. have reported that hydrogen peroxide (H_2O_2) caused significant oxidative etching of Pt-deposited highly oriented pyrolytic graphite (HOPG) accompanied by aggregations of Pt particles while the oxidative etching was not observed in the HOPG without Pt.[9]

ORR on Pt in alkaline electrolyte solutions tends to produce more HO_2^- than in acid electrolyte solutions.[11] In addition, ORR usually proceeds via two-step reactions (namely, 2-electron reduction of oxygen on carbon (Eq. 3) and catalytic disproportionation reaction of hydrogen peroxide on the loaded catalysts (Eq. 4)) in air electrodes loading transition metal oxide catalysts since most of the transition metal oxide catalysts do not have 4-electron ORR activity.[7,12–14]

$$2HO_2^- = O_2 + 2OH^- \quad (4)$$

Therefore, the amounts of hydrogen peroxide produced by ORR should be more significant in alkaline air electrodes than in acid air electrodes. However, the impact of hydrogen peroxide on carbon corrosion in alkaline electrolyte solutions has not been investigated yet.

In this study, we investigate the chemical carbon corrosion reactions by hydrogen peroxide in an alkaline electrolyte solution. We chose HOPG as a model carbon support since its smooth surface and high orientation have an advantage in surface observations. We analyzed the surfaces of HOPG and catalyst-deposited HOPG samples after the immersion test to KOH solution containing hydrogen peroxide by field-emission scanning electron microscopy (FE-SEM) and X-ray photoelectron spectroscopy (XPS).

2. Experimental

2.1 Preparations of HOPG samples

Commercial HOPG (ZYH grade, Momentive Performance Materials Quartz) was carefully cleaved with scotch tape before the measurements. Pt, Ag, MnO_x, and CoO_x were electrochemically deposited on the basal planes of HOPGs under the conditions summarized in Table S1 of the Supporting Information. An electrochemical three-electrode cell composed of a HOPG as the working electrode, a Pt mesh as the counter electrode, and Ag|AgCl|sat'd KCl as the reference electrode was used for the electrodepositions where the geometric surface area of the HOPG was fixed at 0.25 cm^2 by O-ring. Hereafter we describe the catalyst-deposited HOPGs as Pt|HOPG, Ag|HOPG, MnO_x|HOPG, and CoO_x|HOPG, respectively. Characterizations of the prepared samples were carried out by FE-SEM (Hitachi, SU8200) and XPS (ULVAC-PHI, 5500MT). The XPS spectra were measured at room temperature using Mg $K\alpha_{1,2}$ radiation (15 kV, 400 W), and the electron take-off angle was set at 45°. A non-linear least-squares curve-fitting program (MultiPak, Version 8.0) was used to analyze the resultant spectra. Deconvolution of the C1s peak was carried out following the report by Gardner et al. to obtain the distribution of oxygen-containing functional groups.[15]

2.2 Carbon corrosion tests

The HOPG samples were immersed to aqueous solutions of 1.0 mol dm^{-3} KOH + 5 mmol dm^{-3} H_2O_2 saturated with Ar for 15 h to evaluate the impact of hydrogen peroxide on carbon corrosion. The Pt|HOPG was also immersed to an aqueous solution of 0.5 mol dm^{-3} H_2SO_4 + 5 mmol dm^{-3} H_2O_2 saturated with Ar for 15 h to compare the chemical carbon corrosion activities between alkaline and acid electrolyte solutions. Potential holding tests at 0.118 V vs. Hg|HgO (1.00 V vs. RHE) in aqueous solutions of 1.0 mol dm^{-3} KOH saturated with Ar were also performed for 50 h to investigate the electrochemical carbon corrosion. These tests were carried out in an electrochemical three-electrode cell composed of HOPG samples as the working electrodes, carbon paper as the counter electrode, and Hg|HgO as the reference electrode, where the geometric surface areas of HOPG samples were defined at 0.25 cm^2 by O-ring as with the electrodepositions. After the tests, the samples were characterized by FE-SEM and XPS. All the measurements were conducted at room temperature: 25 ± 1 °C.

3. Results and Discussion

3.1 Characterization of the HOPG samples

The FE-SEM images of the prepared HOPG samples show the deposited catalyst particles on the HOPG surfaces (Fig. S1). The mean particle diameters and the coverage rates of the catalyst particles are analyzed with ImageJ software[16] (Table S2 of the Supporting Information). The mean particle diameters are in a range of 60–300 µm, and the coverage rates are in a range of 14–21 %. The depositions of the catalysts are also confirmed by XPS Pt4f, Ag3d, Mn2p, and, Co2p spectra (Fig. S2). The peak of Pt4f (71 eV) and Ag3d (368 eV) spectra indicate the deposition of metallic Pt and Ag. The satellite peaks observed in the Co2p spectrum suggest that the deposited CoO_x particles are $Co(OH)_2$.[17] Though it is difficult to identify MnO_x only from the Mn2p spectrum, we deduce that the deposited MnO_x is MnOOH considering the previous report, in which MnO_x have been deposited with a similar procedure.[18] It is found from XPS C1s spectra that the catalyst depositions did not cause significant changes in the oxygen-containing functional group distributions (Fig. S3).

3.2 Impact of hydrogen peroxide on HOPG and Pt|HOPG corrosions

The FE-SEM images and the distribution of oxygen-containing functional groups of the HOPG without catalyst and Pt|HOPG before and after the immersion test are shown in Figs. 1 and 2. The FE-SEM images of the HOPG without catalyst do not show significant change after the test. In addition, the XPS C1s spectra of the HOPG without catalyst show relatively slight increase of COO functional groups. These results show that further carbon oxidation than C=O functional groups formation is relatively slow in the case of the uncatalyzed chemical carbon corrosion by hydrogen peroxide.

In contrast, the SEM images and XPS C1s spectra of the Pt|HOPG show the formation of some scars and COO functional groups after the immersion test, which indicates that Pt catalyzes the chemical carbon corrosion by hydrogen peroxide to form CO_3^{2-}. In addition, FE-SEM image exhibits the aggregations of Pt particles to form line shapes, where the mean particle diameter of Pt changes from 60 nm to 120 nm, and the scars are mainly observed between the lines. A similar phenomenon has been reported in the acid electrolyte solution, and it has been proposed that Pt particles etched the step edge of the HOPG and moved to aggregate, leaving the scars behind.[9]

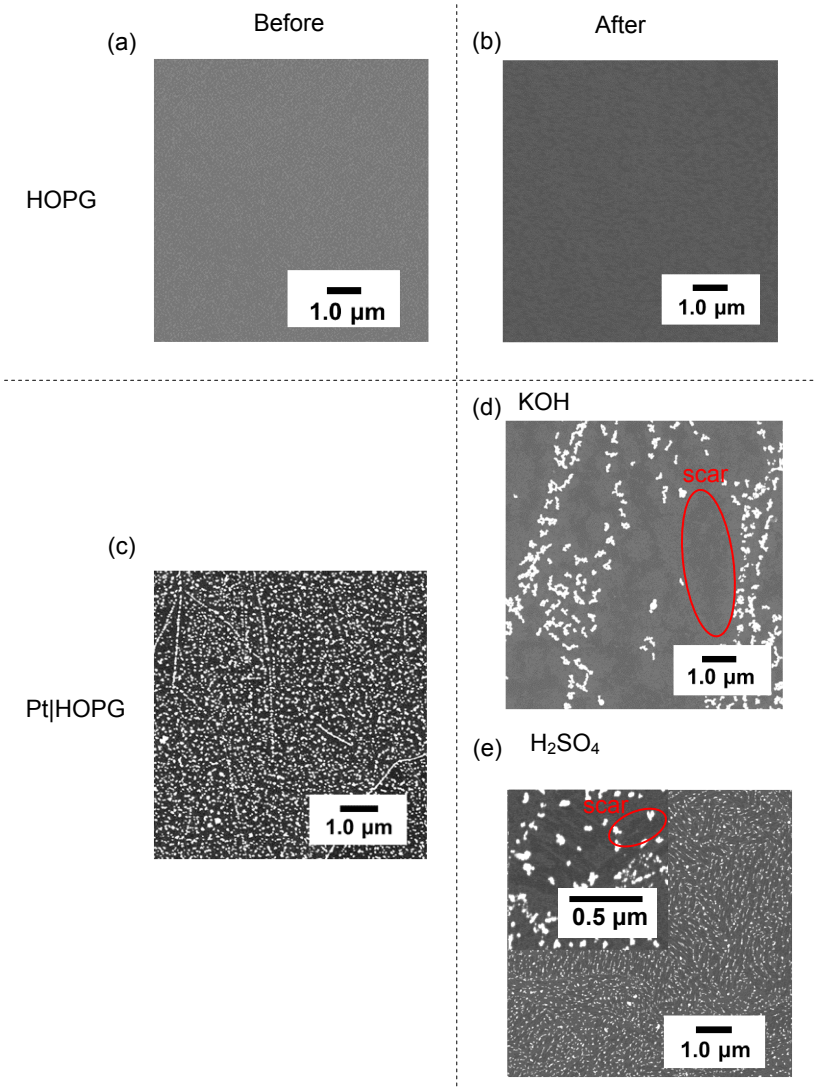

Figure 1. SEM images of (a, b) HOPG and (c–e) Pt|HOPG (a, c) before and (b, d, e) after the immersion test in (b, d) 1.0 mol dm^{-3} KOH + 5 mmol dm^{-3} H_2O_2 and (e) 0.5 mol dm^{-3} H_2SO_4 + 5 mmol dm^{-3} H_2O_2.

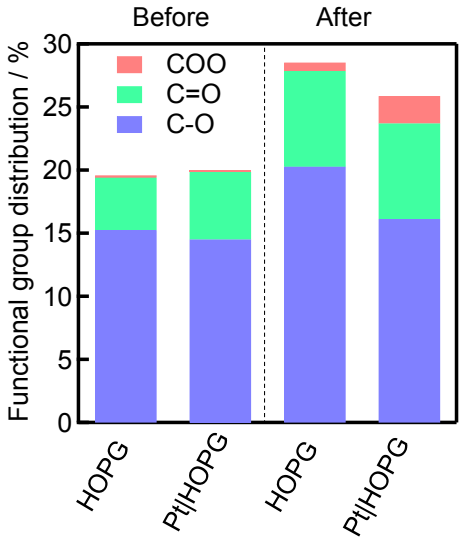

Figure 2. Distribution of oxygen-containing functional groups on HOPG and Pt|HOPG before and after the immersion test in 1.0 mol dm^{-3} KOH + 5 mmol dm^{-3} H_2O_2 calculated from the XPS C1s spectra.

We also carried out the immersion test of the Pt|HOPG to 0.5 mol dm^{-3} H_2SO_4 + 5 mmol dm^{-3} H_2O_2 solution to compare the chemical carbon corrosion activity between the alkaline and acid electrolyte solutions. The change in the FE-SEM images after the immersion test to the acid electrolyte solution is much smaller than that to the alkaline electrolyte solution, while some scars can be observed in the more magnified FE-SEM image (Fig. 1e), which show that the catalytic activity of Pt for the chemical carbon corrosion is much stronger in the alkaline electrolyte solution.

3.3 Impact of hydrogen peroxide on Ag|HOPG, MnO_x|HOPG, and CoO_x|HOPG corrosions

Figures 3 and 4 shows the SEM images and distributions of oxygen-containing functional groups of the Ag|HOPG, MnO_x|HOPG, and CoO_x|HOPG before and after the immersion test. Though Ag|HOPG exhibits many scars around the Ag particles and the increase of COO functional groups, the sizes of the scars are much smaller than that on the Pt|HOPG, suggesting that Ag has lower chemical carbon corrosion activity than Pt. In contrast, scars are hardly observed in the FE-SEM images of the MnO_x|HOPG and CoO_x|HOPG, and the increases of the COO functional groups on the MnO_x|HOPG and CoO_x|HOPG were at the same extent as that on the HOPG without catalyst. In addition, the increases of the oxygen functional groups on the catalyst-loaded HOPGs are lower than that

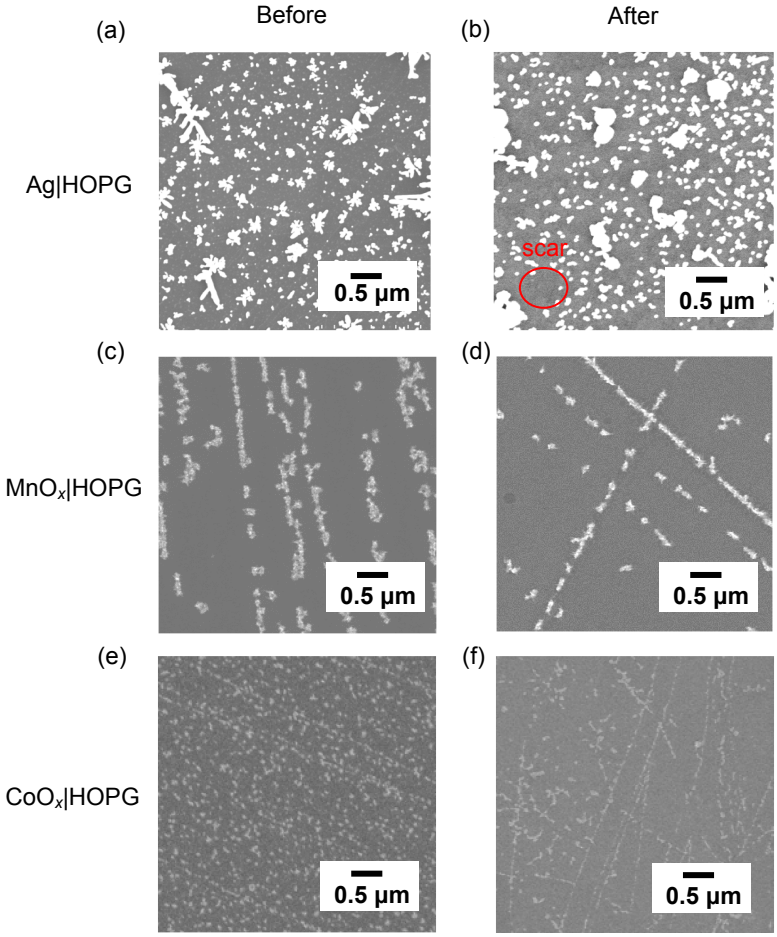

Figure 3. SEM images of (a, b) Ag|HOPGs, (c, d) MnO_x|HOPG, and (e, f) CoO_x|HOPG (a, c, e) before and (b, d, f) after the immersion test in 1.0 mol dm^{-3} KOH + 5 mmol dm^{-3} H_2O_2.

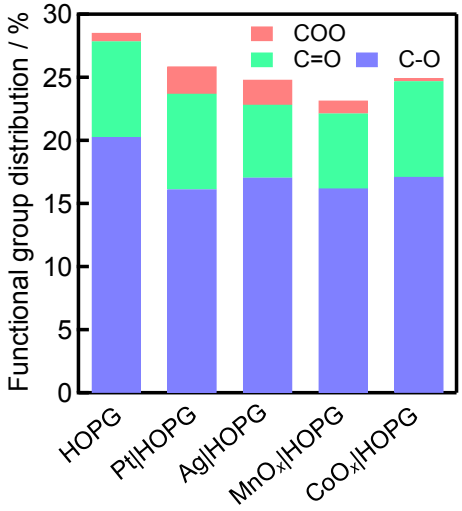

Figure 4. Distribution of oxygen-containing functional groups on the HOPG and catalyst-loaded HOPGs after the immersion test in 1.0 mol dm^{-3} KOH + 5 mmol dm^{-3} H_2O_2 calculated from XPS C1s spectra.

on the HOPG without catalyst (Figs. 2 and 4), which is probably because the direct reaction of HOPG and hydrogen peroxide was suppressed due to the decomposition of hydrogen peroxide on the catalyst. From these results, we can conclude that MnO_x and CoO_x have negligible chemical carbon corrosion activities and can suppress the chemical carbon corrosion by hydrogen peroxide.

3.4 Proposed origin of the difference in the chemical carbon corrosion activity

From the above results, it can be concluded that the chemical carbon corrosion activity is strong in the following order; Pt > Ag > $MnO_x \approx CoO_x$. One of the possible origins of this difference is the electrochemical carbon corrosion activity. Therefore, we performed the potential holding test at 1.0 V vs. RHE to compare the electrochemical carbon corrosion activities of these catalysts. Figure 5 shows the SEM images of the catalyst-loaded HOPGs after the potential holding test. The FE-SEM images of the MnO_x|HOPG and CoO_x|HOPG show several scars, while those of Pt|HOPG and Ag|HOPG show almost no change, which indicates that MnO_x and CoO_x have higher electrochemical carbon corrosion activity than Pt and Ag in contrast to the chemical carbon corrosion activity.

The possible explanation of the difference between the chemical and electrochemical carbon corrosion activity is the lower electron conductivity of the MnO_x and CoO_x. In the case of Pt and Ag, which have relatively high electron conductivity, the electron consumed by the hydrogen peroxide reduction reaction (Eq. 5) at the catalyst|electrolyte interface can be easily transported from the catalyst|carbon interface, where the carbon corrosion reaction occurs (Fig. 6a).

$$HO_2^- + H_2O + 2e^- = 3OH^- \quad E^0 = 0.867\,\text{V vs. SHE} \quad (5)$$

In contrast, higher electronic resistance between the catalyst|electrolyte and catalyst|carbon interfaces could inhibit the chemical carbon corrosion reaction to promote the disproportionation reaction of hydrogen peroxide (Eq. 4) in the case of MnO_x|HOPG and CoO_x|HOPG (Fig. 6b).

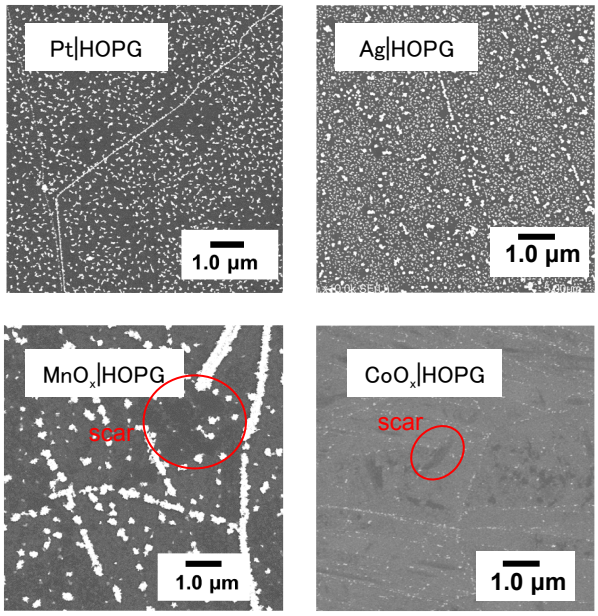

Figure 5. SEM images of (a) Pt|HOPG, (b) Ag|HOPG, (c) MnO_x|HOPG, and (d) CoO_x|HOPG after the potential holding test.

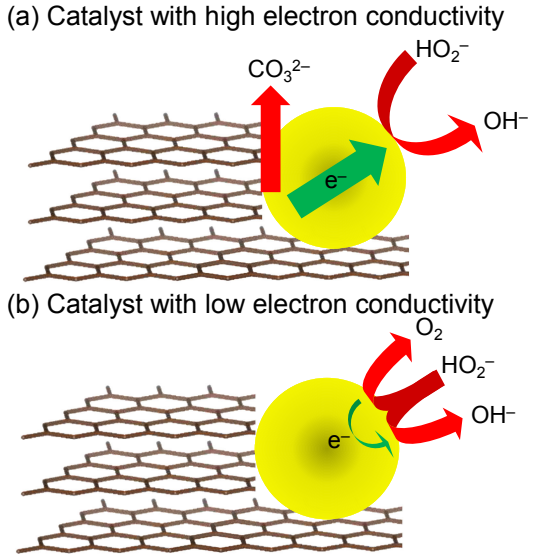

Figure 6. Schematic illustrations of the hydrogen peroxide decomposition reactions on the carbons loading the catalysts with (a) high electron conductivity and (b) low electron conductivity.

4. Conclusion

Impact of hydrogen peroxide on carbon corrosion is investigated by the immersion test of the HOPG samples. While further carbon corrosion than C=O functional group formation was slow in the direct reaction between hydrogen peroxide and HOPG, Pt and Ag catalyzed the chemical carbon corrosion reaction to form the COO functional groups and CO_3^{2-}. In addition, the catalytic activity of Pt for the chemical carbon corrosion was higher in the alkaline electrolyte solution than in the acid electrolyte solution. Considering that ORR on Pt tends to produce more hydrogen peroxide in alkaline electrolyte solutions than in acid electrolyte solutions, it can be deduced that hydrogen peroxide has a more significant impact on the degradation of alkaline air electrodes loading Pt than that of acid air electrodes. In contrast, MnO_x and CoO_x suppressed the chemical carbon corrosion reaction probably because of their low electron conductivity, suggesting that hydrogen peroxide has little impact on air electrodes loading transition metal oxide catalysts. On the other hand, MnO_x and CoO_x have higher electrochemical carbon corrosion activities than Pt and Ag. The use of transition metal oxide catalysts with low electrochemical carbon corrosion activities could improve the durability of air electrodes.

CRediT Authorship Contribution Statement

Atsunori Ikezawa: Investigation (Lead), Writing – original draft (Lead)
Kohei Miyazaki: Project administration (Lead), Supervision (Lead), Writing – review & editing (Lead)
Tomokazu Fukutsuka: Supervision (Equal)
Takeshi Abe: Project administration (Lead), Supervision (Equal)

Data Availability Statement

The data that support the findings of this study are openly available under the terms of the designated Creative Commons License in J-STAGE Data listed in D1 of References.

Conflict of Interest

The authors declare no conflict of interest in the manuscript.

References

D1. A. Ikezawa, K. Miyazaki, T. Fukutsuka and T. Abe, *J-STAGE Data*, https://doi.org/10.50892/data.electrochemistry.17149778, (2021).
1. F. Bidault, D. J. L. Brett, P. H. Middleton, and N. P. Brandon, *J. Power Sources*, **187**, 39 (2009).
2. I. Moussallem, J. Jörissen, U. Kunz, S. Pinnow, and T. Turek, *J. Appl. Electrochem.*, **38**, 1177 (2008).
3. L. Jörissen, *J. Power Sources*, **155**, 23 (2006).
4. T. Tomantschger and R. Findlay, *J. Power Sources*, **39**, 21 (1992).
5. P. Pei, K. Wang, and Z. Ma, *Appl. Energy*, **128**, 315 (2014).
6. T. Morimoto, K. Suzuki, T. Matsubara, and N. Yoshida, *Electrochim. Acta*, **45**, 4257 (2000).
7. H. Arai, S. Müller, and O. Haas, *J. Electrochem. Soc.*, **147**, 3584 (2000).
8. K. Kinoshita, *Carbon*, John Wiley & Sons, New York, p. 334 (1988).
9. T. Kinumoto, K. Takai, Y. Iriyama, T. Abe, M. Inaba, and Z. Ogumi, *J. Electrochem. Soc.*, **153**, A58 (2006).
10. W. C. Schumb, C. N. Satterfield, and R. L. Wentworth, in *Hydrogen Peroxide*, Reinhold Publishing Company, New York, p. 402 (1955).
11. N. Ramaswamy and S. Mukerjee, *J. Phys. Chem. C*, **115**, 18015 (2011).
12. E. Yeager, *J. Mol. Catal.*, **38**, 5 (1986).
13. S. Malkhandi, P. Trinh, A. K. Manohar, K. C. Jayachandrababu, A. Kindler, G. K. Surya Prakash, and S. R. Narayan, *J. Electrochem. Soc.*, **160**, F943 (2013).
14. Y. Miyahara, K. Miyazaki, T. Fukutsuka, and T. Abe, *J. Electrochem. Soc.*, **161**, F694 (2014).
15. S. D. Gardner, C. S. K. Singamsetty, G. L. Booth, and G.-R. He, *Carbon*, **33**, 587 (1995).
16. C. A. Schneider, W. S. Rasband, and K. W. Eliceiri, *Nat. Methods*, **9**, 671 (2012).
17. J. Yang, H. Liu, W. N. Martens, and R. L. Fost, *J. Phys. Chem. C*, **114**, 111 (2010).
18. M. S. El-Deab and T. Ohsaka, *Angew. Chem., Int. Ed.*, **45**, 5963 (2006).